

# Role of Coated Vesicles, Microfilaments, and Calmodulin in Receptor-mediated Endocytosis by Cultured B Lymphoblastoid Cells

J. L. SALISBURY, J. S. CONDEELIS, and P. SATIR

*Department of Anatomy, Albert Einstein College of Medicine, Bronx, New York 10461*

**ABSTRACT** Cell surface receptor IgM molecules of cultured human lymphoblastoid cells (WiL2) patch and redistribute into a cap over the Golgi region of the cell after treatment with multivalent anti-IgM antibodies. During and after the redistribution, ligand-receptor clusters are endocytosed into coated pits and coated vesicles.

Morphometric analysis of the distribution of ferritin-labeled ligand at EM resolution reveals the following sequence of events in the endocytosis of cell surface IgM: (a) binding of the multivalent ligand in a diffuse cell surface distribution, (b) clustering of the ligand-receptor complexes, (c) recruitment of clathrin coats to the cytoplasmic surface of the cell membrane opposite ligand-receptor clusters, (d) assembly and (e) internalization of coated vesicles, and (f) delivery of label into a large vesicular compartment, presumably partly lysosomal. Most of the labeled ligand enters this pathway. The recruitment of clathrin coats to the membrane opposite ligand-receptor clusters is sensitive to the calmodulin-directed drug Stelazine (trifluoperazine dihydrochloride). In addition, Stelazine inhibits an alternate pathway of endocytosis that does not involve coated vesicle formation. The actin-directed drug dihydrocytochalasin B has no effect on the recruitment of clathrin to the ligand-receptor clusters and the formation of coated pits and little effect on the alternate pathway, but this drug does interfere with subsequent coated vesicle formation and it inhibits capping. Cortical microfilaments that decorate with heavy meromyosin with constant polarity are observed in association with the coated regions of the plasma membrane and with coated vesicles. SDS-polyacrylamide gel electrophoresis analysis of a coated vesicle preparation isolated from WiL2 cells demonstrates that the major polypeptides in the fraction are a 175-kdalton component that comigrates with calf brain clathrin, a 42-kdalton component that comigrates with rabbit muscle actin and a 18.5-kdalton minor component that comigrates with calmodulin as well as 110-, 70-, 55-, 36-, 30-, and 17-kdalton components. These results clarify the pathways of endocytosis in this cell and suggest functional roles for calmodulin, especially in the formation of clathrin-coated pits, and for actin microfilaments in coated vesicle formation and in capping.

The cell surface plays an important role in the control of cell proliferation, growth, behavior, and differentiation. Cellular response to external factors is often mediated through the binding of a ligand to its specific cell surface receptor followed by endocytosis. Although the details of how cells deal with ligand-receptor complexes vary, a fundamental pathway is starting to emerge. This pathway involves the association of clathrin coats with the cytoplasmic surface of membrane containing specific receptors, the invagination of these coated membranes, and finally the formation of coated vesicles within

the cell (16, 40, 41). Many receptors are originally diffuse in the membrane before ligand challenge but some, including low-density-lipoprotein receptors, may not be (5, 15-17, 34). For the former, patching or clustering in the plane of the membrane may precede association with the coat and endocytosis. In certain specialized cells, including human lymphocytes, some surface determinants redistribute further after patching in the energy-dependent process known as capping. Endocytosis is known to accompany capping (46), but until the present study it was not known that internalization was, at least

in part, by way of the coated vesicle pathway.

The relation of a ligand-receptor patch to the cell cytoskeleton, particularly the actin-based microfilament system, also has not been clarified. Presumably, such a relationship is important for subsequent capping or endocytosis (but see references 2 and 3). There is both indirect (8, 39, 43) and direct experimental evidence (12, 14) for the association of microfilaments with clustered ligand-receptor complexes.

Using a human B lymphoblastoid cell line (WiL2), we have studied the mobility and endocytosis of the surface-bound IgM-ligand complex in these cells. We show that this involves the clathrin-coated vesicle system and the actin microfilament system in the cell cortex. The interactions between receptor-ligand complexes, coated vesicles, and microfilaments have been analyzed in four ways: (a) by reconstruction of the sequence of endocytosis from light and electron micrographs, (b) by morphometric analysis of ligand distribution after stimulation and inhibition of endocytosis, using specific inhibitors such as Stelazine and dihydrocytochalasin B (dhCB), (c) by direct visualization of heavy meromyosin-labeled actin filaments associated with coated membranes, and (d) by direct isolation of a coated vesicle fraction and analysis of the proteins associated with this fraction.

## MATERIALS AND METHODS

Cultures of the human B lymphoblastoid cell line WiL2 (28) were grown to a density of  $1.5 \times 10^6$  cells/ml in RPMI medium supplemented with 1 mM glutamine and 20% fetal calf serum (Flow Laboratories, Inc., Rockville, Md.) at 37°C and 5% CO<sub>2</sub> in air. Washed cells were resuspended to  $5 \times 10^7$  cells/ml in HEPES (pH 7.4) buffered Hanks' medium with 5% fetal calf serum at 4°C. Surface IgM was labeled, using sandwich technique, with rabbit Ig antihuman IgM ( $\mu$ -chain specific; N. L. Cappel Laboratories Inc., Cochranville, Pa.) followed by three washes in 10 vol of buffer and then with goat antirabbit IgG. The secondary antibody was conjugated with either fluorescein or ferritin (N. L. Cappel Laboratories), or was radioiodinated with <sup>125</sup>I, using the chloramine-T method (7). After the cells were washed free of unbound antibody, the suspension was warmed to 37°C for varying periods of time.

Uptake of horseradish peroxidase was measured according to the methods outlined by Steinman (45).

Heavy meromyosin (HMM) was made from rabbit muscle myosin according to Lowey and Cohen (33). Cellular actin was decorated with HMM after glycerination according to Ishikawa et al. (20).

Cells were fixed for electron microscopy at room temperature with 2% glutaraldehyde in phosphate buffer (pH 7.0) with or without 0.1% tannic acid (6) for 1 h and postfixed at 4°C with 1% OsO<sub>4</sub> in phosphate buffer (pH 6.0) for 20 min. The material was dehydrated in an ethanol series, infiltrated with Epon 812, thin sectioned, stained with uranyl acetate and lead citrate or bismuth subnitrate (1), and observed on a Siemens 101 electron microscope operated at 80 kV.

Analysis of the distribution of ferritin-labeled ligand-receptor clusters relative to membrane cytoplasmic specializations (membrane coats) was carried out according to the stereological principles for morphometry outlined by Weibel (49). Sample selection was randomized by sectioning multiple blocks and levels within the pellets of cells from each treatment. Sections (silver interference colors) were mounted on 200-mesh grids, stained with bismuth subnitrate (1), and viewed with the electron microscope at  $\times 6,000$  magnification without the aid of binoculars. Under these conditions, neither ferritin clusters nor membrane specializations can be discerned. Cell profiles that included nuclear cross sections were chosen from the upper left or lower right corner of a given grid hole, centered, focused with the aid of binoculars, and photographed. Electron micrographs were printed at a final magnification of  $\times 42,000$ . The prints were then analyzed by point-counting planimetry for volumetric analysis and differential intersection counting for estimation of fractional boundaries for cell surface specialization. Raw data total 77,779 points and 12,134 linear intercepts from 480 electron micrograph prints at  $\times 42,000$  magnification. Calculations are based on an average cell surface area of  $300 \mu\text{m}^2$ , an average coated vesicle membrane surface area of  $7.2 \times 10^3 \text{ nm}^2$ , and an estimated section thickness of 750 Å.

Coated vesicles were isolated by a modification (23) of the Pearse (38) procedure from WiL2 cells that were actively endocytosing at 37°C just before cell lysis. Clathrin standards for SDS-polyacrylamide gel electrophoresis (SDS-PAGE) were prepared from calf brain coated vesicles after a single cycle of depolymerization in 0.5 M Tris buffer (pH 7.5) and basket reassembly from an

85,000  $\times g$  supernate by dialysis against the isolation buffer.

SDS-PAGE was carried out in 5–15% gradient polyacrylamide gels containing 0.1% SDS, using the buffer system of Laemmli (25).

Drug treatments were for 15 min before fixation with either 20  $\mu\text{M}$  dhCB (substoichiometric relative to cell actin [J. Carboni and J. Condeelis, unpublished observation]) or 25  $\mu\text{M}$  Stelazine (trifluoperazine dihydrochloride; Smith, Kline and French Labs, Philadelphia, Pa.). dhCB has been shown to be quite specific for actin-related motility processes and has little or no effect on glucose transport (29, 31). The cytochalasins inhibit *in vitro* polymerization and reduce the rate of elongation of actin filaments when applied at substoichiometric concentrations relative to actin (9, 10, 30). Stelazine, a phenothiazine derivative, is a potent and highly specific inhibitor of calmodulin-mediated regulation (19, 27, 50). Stelazine binds with high affinity to the calcium-dependent regulator in the presence of calcium and inactivates calmodulin in the brain phosphodiesterase stimulation assay (27, 50), in the adenylate cyclase stimulation assay (50), and in regulation of smooth muscle contraction (19).

## RESULTS

### Redistribution and Endocytosis

WiL2 cells patch and cap fluorescein-labeled Ig-IgM complexes. After challenge with fluorescein-labeled anti-IgM antibody, the cells initially display a diffuse pattern of cell surface labeling (Fig. 1a). Patches develop within minutes and when the cells are warmed to 37°C these ligand clusters rapidly gather into a cap over one pole of the cell (Fig. 1b). In a typical experiment, 50% of the cells have a polar distribution of label over less than half their cell surface within 15 min of raising the temperature, whereas the rest of the surface is devoid of label. 80–90% of the cells display this type of distribution by 30 min.

For EM study at higher resolution, ferritin-labeled antibody has been used so that ligand is indicated by the electron opaque ferritin. When cells are maintained and fixed at 4°C, the ferritin is observed dispersed more or less uniformly along the cell membrane (Fig. 2a). When the cells are warmed to 37°C, the ferritin label redistributes into a cap over the Golgi region of the cell. A typical thin section of the capped region of a cell fixed 15 min after challenge is shown in Fig. 2b. By this time, numerous channels filled with ferritin penetrate the cell cortex, suggesting that endocytosis of the bound ligand has begun.

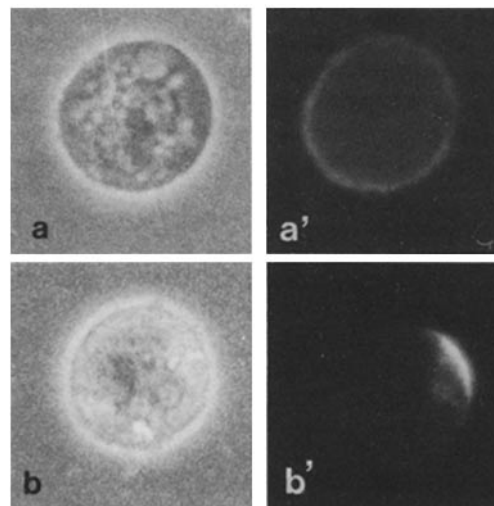


FIGURE 1 Distribution of WiL2 cell surface receptor IgM before and after capping. (a) Cell fixed immediately after labeling with rabbit antihuman IgM and fluorescein-conjugated goat antirabbit antibodies. The labeled receptor IgM is located in a diffuse cell surface distribution. (b) Cell fixed after 15-min incubation at 37°C, postlabel. The receptor IgM has redistributed into a cap. a and b: Phase; a' and b' fluorescence image.  $\times 2,000$ .

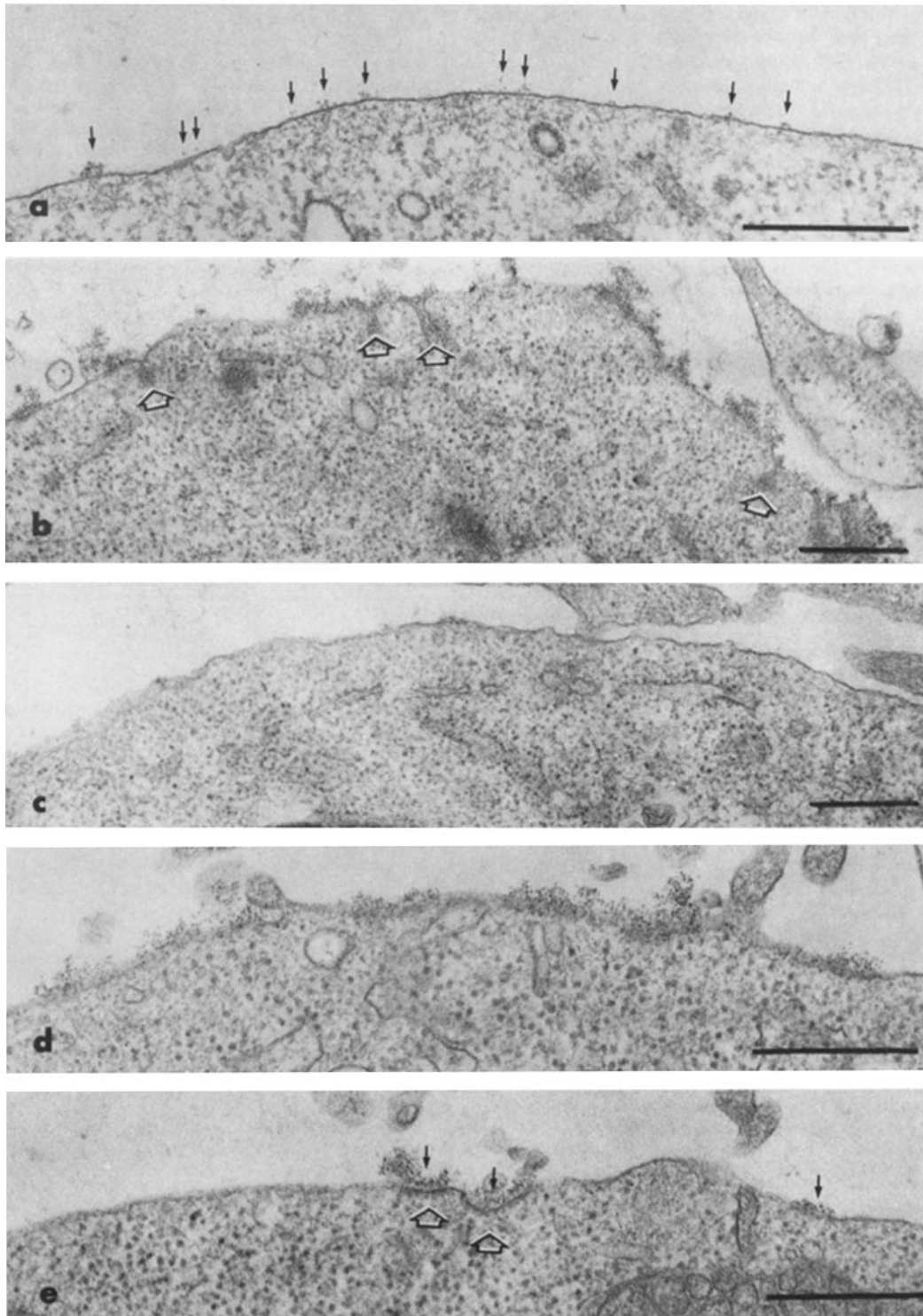


FIGURE 2 Distribution of WIL2 cell surface receptor IgM at ultrastructure resolution, using ferritin-conjugated secondary antibody. (a) Cell fixed immediately after antibody labeling shows a diffuse cell surface distribution of ferritin label (arrows) with few clustered receptors. Stain: uranyl acetate followed by bismuth subnitrate. (b) Cell fixed after 15-min incubation at 37°C, postlabel. The label was redistributed into a cap. Beneath the cap, numerous channels filled with ferritin penetrate the cell cortex (arrows), suggesting that endocytosis of bound ligand has begun. Stain: uranyl acetate followed by lead citrate. (c) A region of the same capped cell as in b that has been cleared of its cell surface IgM. (d) Cell treated with Stelazine (25  $\mu$ M), fixed after 15-min incubation at 37°C, postlabel. The ligand has capped normally but endocytic channels are absent. Stain: bismuth subnitrate. (e) Cell treated with dhCB (20  $\mu$ M), fixed after 15-min incubation at 37°, postlabel. The ferritin-labeled ligand-receptor complexes cluster normally but do not cap. The clustered receptors (arrows) associate with clathrin coats (open arrows) but internalization is reduced. Stain: bismuth subnitrate. Bars, 0.5  $\mu$ m. a, d, and e:  $\times$  48,000; b and c:  $\times$  31,000.

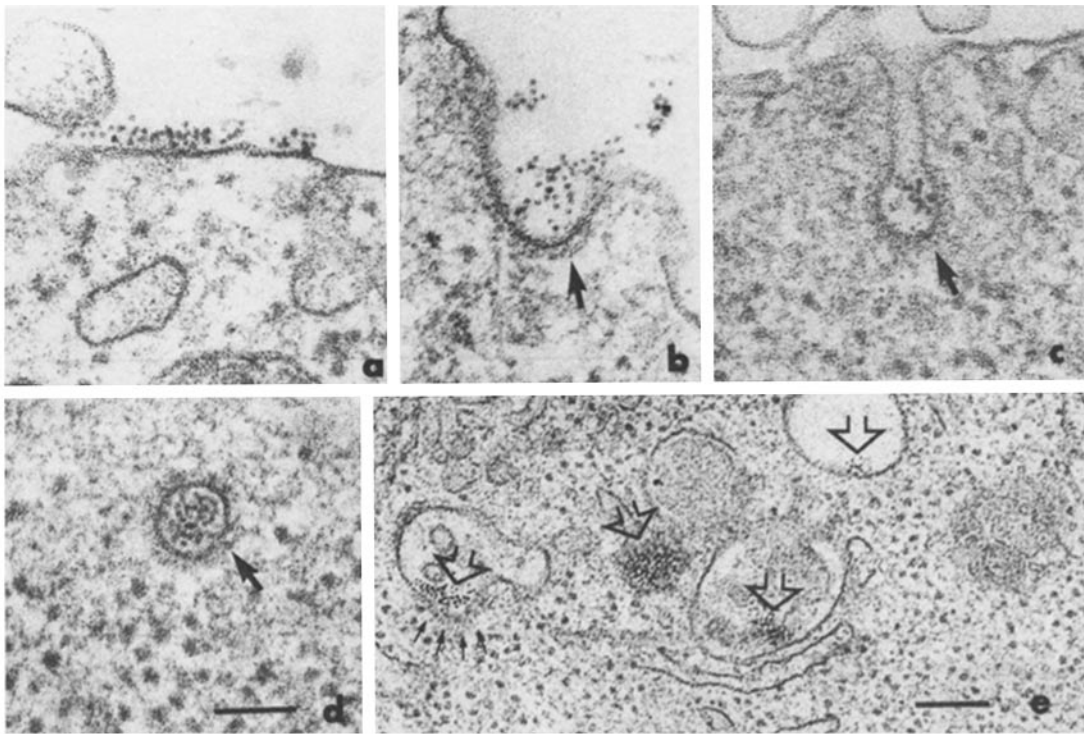


FIGURE 3 Cell surface receptor IgM is internalized along a coated vesicle pathway of endocytosis. (a) At high magnification of a capped cell, the ligand often appears in small separate clusters over straight or slightly convex expanses of plasma membrane without underlying cytoplasmic coats. (b) Some clusters are observed over indented regions of the plasma membrane that clearly have coats on their cytoplasmic surface (arrow). (c) Ferritin clusters also occur in deep coated depressions or pits; the coated region (arrow) is at the end of a long channel. (d) Also, the ligand is observed in the cytoplasm beneath the cap within coated vesicle profiles of  $\sim 100$ -nm diameter, and (e) within larger uncoated structures (open arrows) of approximately 0.2- to 0.4- $\mu\text{m}$  diameter. Some of these larger structures have features of lysosomes (see text). Other large vesicles with ferritin label do not have these features. a–d: bar, 0.1  $\mu\text{m}$ ,  $\times 100,000$ , e: bar, 0.2  $\mu\text{m}$ ,  $\times 50,000$ .

At higher magnification of capped cells, the ligand often appears in small separate clusters over straight or slightly convex expanses of the plasma membrane without underlying cytoplasmic coats (Fig. 3a). Some clusters are observed over indented regions of the plasma membrane that clearly have coats on their cytoplasmic surface (Fig. 3b). Clusters also occur in deep coated depressions or coated pits (Fig. 3c). Finally, ligand is observed in the cytoplasm beneath the cap in the Golgi region of the cell within coated vesicle profiles  $\sim 100$  nm in diameter (Fig. 3d) and within large uncoated structures of  $\sim 0.2$ – $0.4$   $\mu\text{m}$  in diameter (Fig. 3e). Some of these larger structures have a granular matrix in addition to the ferritin particles and have an electron-transparent halo just beneath their limiting membrane. These features are hallmarks of lysosomes (37) and we will refer to these vesicles as presumptive lysosomes. Other large (0.2–0.4  $\mu\text{m}$  in diameter) vesicles with ferritin label that occur in this region of the cell do not have these features. We postulate that Fig. 3a–d represent the sequence of events in the transport and processing of the cell surface ferritin-labeled ligand via a coated vesicle pathway. In this sequence, coated vesicle formation begins after ligand-receptor patching and continues during and after capping. The sequence ends when coated vesicles presumably fuse with and deposit ligand into presumptive lysosomes (Fig. 3e).

#### Morphometric Analysis of Controls

This postulated pathway is confirmed in the morphometric analysis (Table I). When the cells are fixed immediately after antibody treatment,  $\sim 18$   $\mu\text{m}^2$  or 6% of the total cell surface area (300  $\mu\text{m}^2$ ) is scored as occupied by ferritin-labeled ligand.

The label is dispersed more or less uniformly over the cell surface. 94% of this label is over unspecialized membrane (without cytoplasmic coats), whereas only 5% is over coated membranes. When the cells are warmed to 37°C for 15 min and allowed to cap the ligand,  $\sim 15$   $\mu\text{m}^2$  or 5% of the membrane surface area is scored as occupied by ferritin-labeled ligand. The slight drop in cell membrane scored as occupied by ferritin-labeled ligand is a result of superposition of marker in the thickness of the section because of receptor clustering.

By 15 min of incubation, the ferritin label distribution relative to membrane coats has changed dramatically. After a 15-min incubation, only 35% of the label remains over unspecialized plasma membrane, whereas 36% is over regions of membrane with cytoplasmic coats, 7% is found within coated vesicle profiles and 22% within the presumptive lysosomal compartments. The ligand clusters represent preferred sites of coated pit formation. Within 15 min after ligand challenge, coated pits occupy 2.8% of the total cell surface area (8.4  $\mu\text{m}^2$ ) yet 64% (5.4  $\mu\text{m}^2$ ) of the coated pits contain label. Also by 15 min, ligand challenge has stimulated threefold the number of coated pits formed at the cell surface (2.7  $\mu\text{m}^2$  membrane surface area is coated initially, and 15 min after challenge 8.4  $\mu\text{m}^2$  is coated). This increase in the coated membrane can be accounted for entirely by the recruitment of clathrin coats to the membrane opposite ligand clusters.

#### Effect of Various Treatments on Ligand-Receptor Distribution and Endocytosis

Preliminary studies on endocytosis of exogenous horseradish peroxidase by WiL2 cells indicated that uptake is cold, azide

TABLE I

Effect of Actin- and Calmodulin-directed Drugs on Ligand-Receptor Distribution Relative to Membrane Specializations

	Membrane surface area occupied by ferritin clusters									
	Cell surface				Intracellular				Total	
	Unspecialized membrane		Coated membrane		Coated vesicle profiles		Large vesicles (lysosomes)		Ferritin-labeled membrane	Coated pits ( $\pm$ ferritin)
	$\mu\text{m}^2$	% Total	$\mu\text{m}^2$	% Total	$\mu\text{m}^2$	% Total	$\mu\text{m}^2$	% Total	$\mu\text{m}^2$	
Control, 0 min	17.1	(94)	0.9	(5)	0	(0)	0.2	(1)	18.2	2.7
Control, 15 min	5.1*	(34)	5.4*	(36)	1.0*	(7)	3.3*	(22)	14.8	8.4*
Dihydrocytochalasin B, 15 min	5.6	(39)	6.0	(41)	0.4†	(3)	2.4†	(16)	14.4	8.1
Stelazine, 15 min	11.4†	(73)	3.0†	(19)	0.6	(4)	0.6†	(4)	15.6	5.7†

Based on morphometric analysis according to the methods of Weibel (49), using point planimetry for volumetric analysis and differential intersection counting for estimation of fractional boundaries for cell surface specializations. Calculations based on an average cell surface area of  $300 \mu\text{m}^2$  and coated vesicle membrane surface area of  $7.2 \times 10^3 \text{ nm}^2$  and average section thickness of  $750 \text{ \AA}$ . Student's unpaired *t* test analysis of data distributions indicate significant differences ( $P < 0.05$ ).

\* 15 min control vs. 0 min control.

† 15 min drug treatments vs. 15 min control.

( $10^{-3} \text{ M}$ ), dhCB ( $20 \mu\text{M}$ ) and Stelazine ( $25 \mu\text{M}$ ) sensitive, yet colchicine ( $10^{-5} \text{ M}$ ) and dimethyl sulfoxide (0.1%) insensitive. We chose to study in some detail the effects of Stelazine and dhCB on ligand-receptor distribution and internalization after a 15-min incubation.

Cells that have been treated with  $25 \mu\text{M}$  Stelazine, added at the time of ligand challenge, cap normally within 15 min after warming to  $37^\circ\text{C}$ . However, endocytic channels are rarely seen in the capped regions of these cells (Fig. 2*d*). In the presence of Stelazine, over 90% of the total labeled ligand receptor clusters remain at the cell surface. Nearly 80% of this label is over uncoated regions of the membrane and has not yet entered an endocytic pathway (Table I). The amount of ligand entering an endocytic pathway is reduced by  $>50\%$  of the control values.

A similar reduction also occurs in the number of ligand-labeled coated vesicles scored. This is taken to indicate that once the coat is recruited to the membrane, the percentage of coated pits converted to coated vesicles in 15 min in the presence of Stelazine is the same as the percentage converted in the control. Because the coated vesicles scored are the resultant sum of both those formed and those degraded (by fusion with lysosomes), we assume that the rate of these processes is the same in Stelazine vs. control samples. Thus, Stelazine has an effect on the overall recruitment of coat material to the membrane but not on further processing of the coated vesicles. However, this effect on recruitment does not completely account for the level of inhibition of overall endocytosis seen in the presence of the drug. Note that Stelazine shuts down  $>80\%$  of the transfer of cell surface label into the larger vesicles.

In contrast to Stelazine, dhCB prevents cell capping, although ligand-receptor clustering seems unaffected by dhCB (Fig. 2*e*). Also in contrast to Stelazine, dhCB has little effect on the recruitment of clathrin coats to the cell membrane or on the amount of ferritin-labeled ligand entering the endocytic pathway (Table I). Two-thirds of the total labeled clusters remain at the cell surface and one-half of these clusters lie above coated pits. The number of coated pits formed is about the same in dhCB as in the control, at least within the error of our measurements. Thus we conclude that dhCB has no effect on the recruitment of coats to ligand-receptor clusters and that entry into the coated vesicle pathway in general is therefore

separated from capping in these cells. However, this drug does have an effect on the internalization of the clusters. The number of labeled coated vesicle profiles scored in dhCB-treated preparations is significantly lower than the control values, despite an equivalent amount of membrane entering the endocytotic pathway and an equivalent amount of coated cell surface. The number of coated vesicle profiles scored after dhCB is even lower than the number seen with Stelazine (Table I). We conclude that conversion of coated pits into coated vesicles is inhibited by dhCB.

Despite the fact that fewer coated vesicle profiles are scored after dhCB than after Stelazine treatment, the transfer of labeled ligand into the large vesicular compartment in dhCB is four times greater than after Stelazine. A possible explanation of this finding might be that a second pathway of endocytosis of ligand exists, independent of the coated vesicle pathway. For example, taken from uncoated cell surfaces (Fig. 3*a*) directly to electron-transparent large vesicles may represent an alternate pathway (Fig. 3*e*). Such an explanation is consistent with the conclusions of other workers (13) regarding bulk membrane flow endocytosis in cells. Because Stelazine inhibits overall endocytosis and transfer of label into the large vesicular compartment much more effectively than it inhibits the coated vesicle pathway, we deduce that Stelazine inhibits this second pathway. Because considerable label is present in the large vesicular compartment in dhCB, this drug would seem to have little effect on an alternate pathway. In untreated cells, just over 20% of the total surface label reaches the large vesicular compartment in 15 min after ligand challenge. Based on our observations, the total label found in the presumptive lysosomal compartment would be the sum of labeled membrane derived from both the coated vesicle pathway and alternate pathway.

#### Analysis of Proteins Associated with the Endocytotic Pathway

The drug studies presented above demonstrate that Stelazine and dhCB are effective inhibitors of different processes along the endocytotic pathway. Because inhibitor studies are indirect, we turned to specific labeling and direct isolation to demonstrate the involvement of calmodulin and actin as components of the coated vesicle pathway. These procedures have also

clarified the protein composition of a coated fraction from the WiL2 cell.

**ASSOCIATION OF HMM-DECORATED MICROFILAMENTS WITH COATED PITS AND COATED VESICLES:** The cortical region of the cell is rich in microfilaments that decorate with HMM. These decorated filaments have an arrowhead periodicity of  $\sim 37$  nm and are decorated actin filaments. Together with the microfilaments, many coated regions of the cell membrane and coated vesicles survive the glycerination necessary for HMM labeling, although the cell membrane is permeabilized and the cytoplasm extracted. Frequently, structural associations are observed between ferritin-labeled ligand-receptor patches over uncoated membrane and the ends of decorated microfilaments (Fig. 4*a*). Actin-containing microfilaments also run outward from coated pits and coated vesicles (Fig. 4*a* and *b*). When microfilaments are observed in association with the plasma membrane, the arrowhead polarity of decoration points away from the membrane. This is also true when microfilaments are associated with coated pits or completely formed coated vesicles. The constant polarity of HMM-decorated actin filaments relative to the coated membrane suggests that the actin-membrane association is a specific one.

**ISOLATED COATED VESICLES:** Coated vesicles have been isolated from cells that were actively capping and internalizing ligand-receptor complexes. When cells were challenged with secondary antibody radiolabeled with  $^{125}\text{I}$ , the final coated vesicle fraction retained significant levels of  $^{125}\text{I}$  label. In a typical experiment, 2.3% of the initial  $^{125}\text{I}$  label was recovered in the coated vesicle preparation. From our morphometric studies with ferritin label (Table I), this is the amount of radiolabel one could expect if the isolation procedure resulted in yields of one-third of the initial labeled coated vesicle population. In control experiments, where the primary antibody (anti-IgM) was omitted, no  $^{125}\text{I}$  secondary antibody label (counts above background) was recovered in the final coated vesicle preparation. The isolated coated vesicles (Fig. 5) are generally uniform,  $109 \pm 5$  nm in diameter, and enclose unit membrane vesicles of  $\sim 48 \pm 5$  nm diameter. Some contaminating particles and a few smooth vesicles are also present. Actin microfilaments are not seen, and presumably have largely

been dissociated or depolymerized from the coat during isolation. Thus, by structural criteria, the coated vesicles in these cell fractions are comparable to those obtained by other workers (22, 38).

**PROTEIN PROFILE OF THE COATED VESICLE FRACTION:** One-dimensional SDS-PAGE analysis of the coated vesicle fraction isolated from WiL2 cells is shown in Fig. 6. The major components of the preparation are a polypeptide that comigrates with authentic calf brain clathrin with an apparent molecular mass of 175 kdaltons and a polypeptide that comigrates with authentic rabbit muscle actin with an apparent molecular mass of 42 kdaltons. A minor component of the coated vesicle fraction that comigrates with authentic rat testis calmodulin can be seen at 18.5 kdaltons. Other polypeptide components in the coated vesicle fraction migrate with apparent molecular mass values of 110, 70, 55, 36, 30, and 17 kdaltons. Some of these may be breakdown products of clathrin. Myosin is not present, nor are other muscle proteins except actin. The relative amounts of actin vs. clathrin in such preparations vary, depending upon how the cells are treated before homogenization. For example, if the cells are maintained at  $0^\circ\text{--}4^\circ\text{C}$  for extended periods of time before cell lysis, the amount of actin that copurifies with the coated vesicles is diminished.

## DISCUSSION

Cultures of the human lymphoblastoid cell line WiL2 (28) provide a relatively uniform and homogeneous population of cells. WiL2 cells have immunoglobulin of the IgM class specifically associated with their plasma membrane (24, 26). The cells appear to be arrested at an early stage of differentiation along a B lymphocyte lineage (21, 26, 36), because they do not secrete large quantities of antibody. This system is amenable to morphometric and biochemical characterization of cell surface events, such that a detailed picture of the initial stages of response at the cell surface to a specific ligand challenge can be reconstructed.

IgM originally is dispersed in the WiL2 cell membrane because, when anti-IgM is presented, the multivalent ligand

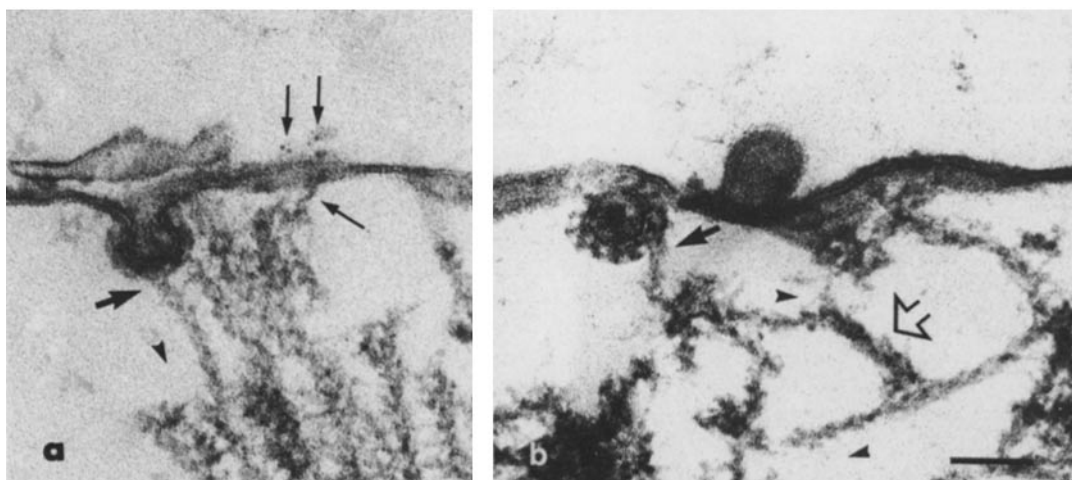


FIGURE 4 Microfilaments are found in association with coated membranes (thick arrows). (a) Structural associations are observed between HMM decorating microfilaments and coated pits. In all instances the polarity of HMM decoration points away from the coated membrane, into the cytoplasm. Similarly, decorated microfilaments are often seen associated with ferritin at the cell surface (thin arrows). (b) This image shows a coated vesicle profile associated with a decorated actin filament that is in turn associated with a second actin filament of opposite polarity by a thicker filament (open arrow). This is the orientation expected for an active involvement of microfilaments in the formation and movement of coated vesicles through the cytoplasm. Bar,  $0.1 \mu\text{m}$ .  $\times 85,000$ .

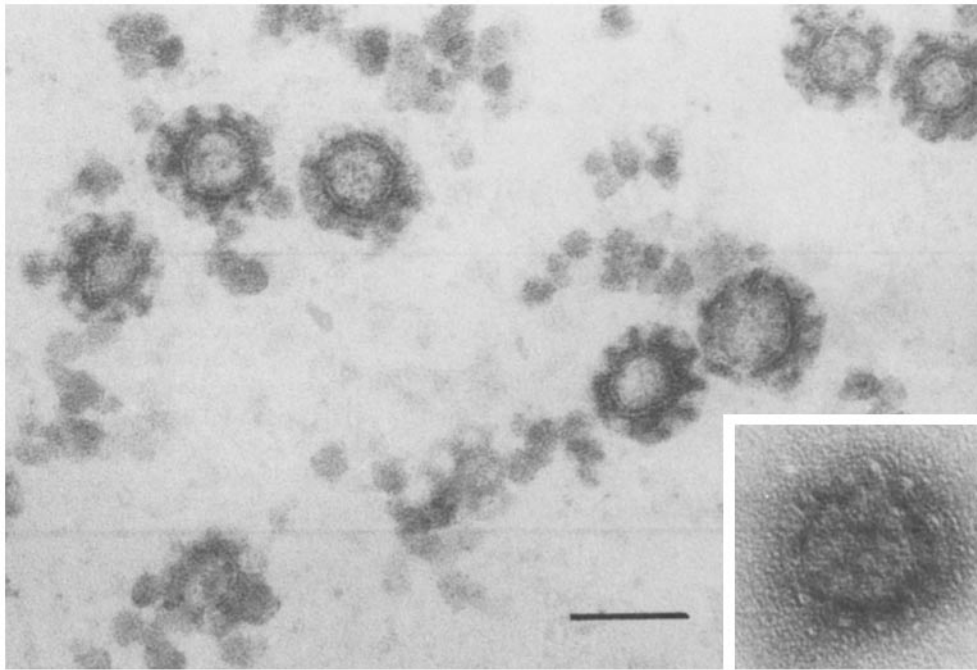


FIGURE 5 Isolated WIL2 coated vesicles. Note that all of the coats surround membrane vesicles; none of the coats are "empty."  $\times 150,000$ . Inset: negatively stained coated vesicle.  $\times 200,000$ . Bar,  $0.1 \mu\text{m}$ .

initially binds with a diffuse distribution. In this paper we have shown that the cell deals with the ligand-receptor complexes formed after antibody challenge by activating a specific endocytic pathway involving the following sequence of events (Fig. 7):

(a) Clustering of the diffuse ligand-receptor complexes (patching). Patch formation is thought to involve receptor mobility in the membrane and to depend on the multivalent nature of the ligand (13, 46). The clustering of ligand-receptor complexes is not sensitive to the drugs employed in this study.

(b) Recruitment of clathrin to the clustered ligand-receptor complexes to form a coated pit. This recruitment occurs in response to ligand-induced receptor clustering, because the amount of cell surface that is coated increases threefold after antibody challenge, and all the new coated pits seen can be accounted for by ferritin-labeled regions of the membrane that have acquired coats. The coat recruitment is Stelazine sensitive and is unaffected by dhCB.

(c) The internalization of the coated pit to form a coated vesicle. This process is dhCB sensitive and is unaffected by Stelazine. The internalized vesicles containing ligand then migrate toward the Golgi-lysosome region of the cell and fuse with the lysosomes.

In addition, there is probably an alternate endocytic pathway in these cells that accounts for a portion of the internalized label. This pathway presumably moves labeled ligand from uncoated cell membrane directly to the large uncoated vesicles in the cytoplasm, and may correspond to a general pinocytotic mechanism described in other systems (13). Most of the labeled ligand enters the coated vesicle pathway. Both the coated vesicle and the alternate pathway are separable from capping of the receptor, which redistributes label further at the cell surface. Our results suggest that in these cells capping may be inhibited without significant inhibition of coated pit formation, and that bulk flow endocytosis may be blocked without inhibiting capping. However, internalization of coated pits and

capping are inhibited simultaneously by dhCB, suggesting that both events, although independent, require actin-microfilament interaction with the ligand-receptor complex.

The sequence of events for receptor-mediated endocytosis via the coated vesicle pathway illustrated in this paper is a general one, although specific details may vary with differing cell types. For example, the lymphocyte response to antibody shares a number of features in common with uptake of epidermal growth factor and insulin in fibroblasts (15, 34) and with uptake of Semliki Forest virus into BHK-21 cells (18).

### Quantitative Considerations regarding Coat Recruitment

Our morphometric analysis shows that, initially,  $\sim 18 \mu\text{m}^2$  or 6% of the total cell surface membrane area is scored as possessing receptor IgM molecules as determined by ferritin-labeled antibody binding. The initially diffuse labeling pattern, however, rapidly changes as ligand-receptor complexes cluster and begin to redistribute in the plane of the membrane. By 15 min after antibody challenge, the membrane scored as ferritin-labeled, in all treatments studied, drops to  $\sim 15 \mu\text{m}^2$  or 5% of the initial cell surface area. This reduction is mainly because of superpositioning of ferritin in the thickness of the sections as a result of receptor clustering. The constancy of ferritin-labeled membrane scored after 15-min incubation is a reflection of the stability of the ligand-receptor complex over time and the absence of any effect of the drug treatments studied on either the number of initially available receptors or on their ability to bind ligand. The amount of total labeled membrane scored after a 15-min incubation is therefore an internal control for the morphometric analysis and is a measure of the sensitivity of the technique.

When cells were fixed for electron microscopy as soon after antibody labeling as possible (our zero time), 94% of the ferritin-label was observed to be over uncoated regions of the

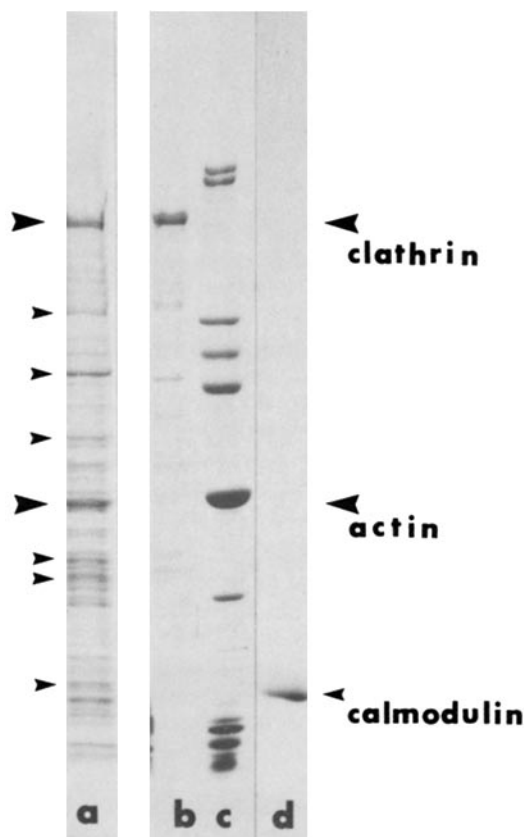


FIGURE 6 SDS-PAGE analysis of coated vesicle proteins. Track a: WiL2 coated vesicle fraction. Arrows indicate major polypeptide components and those polypeptides that are found in coated vesicle fractions from diverse sources. Track b: calf brain coated vesicle clathrin, 175 kdaltons. Track c: polypeptide standards: (top to bottom) *Dictyostelium* myosin heavy chain, 225 kdaltons; rabbit muscle myosin heavy chain, 200 kdaltons; phosphorylase a, 94 kdaltons; human transferrin 78 kdaltons; bovine serum albumin, 68 kdaltons; rabbit muscle actin, 42 kdaltons; concanavalin A, 27 kdaltons; cytochrome c, 11.7 kdaltons. Track d: rat testis calmodulin, 18.5 kdaltons. 5-15% gradient polyacrylamide gel, 0.1% SDS.

cell membrane and 5% over coated pits. Because coated pits occupy ~1% of the cell surface area, at zero time we would expect to see only 1% of the ferritin-label associated with pits if the receptor IgM were randomly distributed. We believe that this discrepancy is attributable to receptor clustering and recruitment of coat material or movement over coats in the short time before and possibly during fixation. There are no ferritin-labeled coated vesicles at this early time after antibody challenge; however, a small amount of label is observed in the large uncoated vesicular compartment. 15 min after ligand challenge, the amount of coated surface membrane has increased to three times the initial value so that ~5-6  $\mu\text{m}^2$  of new coated surface has come into being. As mentioned above, the coat material is recruited quite specifically to the clustered ligand-receptor complexes, so that at this time nearly 40% of all receptor IgM is found associated with coated membrane. This represents an eightfold increase of total ferritin-labeled clusters associated with coated membrane. In contrast, the amount of coated membrane without ferritin label remains unchanged.

The coat material recruited to the membrane is clathrin, by morphological and biochemical criteria. Because the total amount of coat material found increases dramatically upon

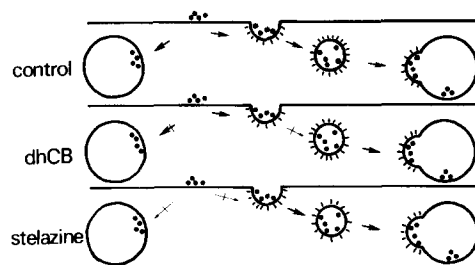


FIGURE 7 This diagram summarizes pathways constructed using data in Table I. *Control*: ferritin-labeled ligand initially binds to the cell surface with a diffuse distribution over regions that do not have clathrin coats. After clustering of the receptors, clathrin recruitment to the cell membrane is stimulated and coated regions form below the clusters. These specialized coated regions invaginate and internalize bits of membrane with ligand in coated vesicles. The ligand is then shuttled to a large vesicular compartment, part of which we have identified as lysosomal by morphological criteria. This sequence represents the coated vesicle pathway of endocytosis. Some portion of the cell surface label is internalized by an alternate, nonspecific, endocytic pathway that does not involve coated vesicles. *dhCB*: dhCB has no apparent effect on clustering of the receptors or association with clathrin coats opposite the ferritin clusters. This drug does, however, significantly reduce the number of coated vesicle profiles scored as well as the amount of label observed in the large vesicular compartment. *Stelazine*: Stelazine has no apparent effect on clustering of the receptors, but this drug does inhibit the association of clathrin coats with the ligand-receptor complexes. Stelazine also shuts down the alternate endocytic pathway almost completely. Major rate reductions are indicated by small blocked arrows; minor rate reductions are indicated by large blocked arrows.

ligand challenge, we believe that clathrin is assembled into coats under the ligand-receptor complex from a cytoplasmic pool, although an alternate source of the newly visualized coating material may be by a rearrangement of a submembrane network of clathrin. In either case, the signal for recruitment or rearrangement appears to be receptor clustering, but the detailed molecular mechanism is not known.

#### *Involvement of Calmodulin in Coat Recruitment and Endocytosis*

The recruitment of coat material to the cytoplasmic side of the membrane opposite ferritin-labeled ligand-receptor clusters is Stelazine sensitive. Stelazine reduces both the amount of labeled coated surface and the number of coated vesicles formed to about 60% of control values by 15 min. This result suggests that calmodulin is an important mediator of clathrin recruitment to the membrane. In support of this conclusion, we find a polypeptide that comigrates with calmodulin associated with coated vesicles isolated from WiL2 cells. Similarly, Linden et al. (32) have used the sensitive radioimmunoassay technique to demonstrate calmodulin in highly purified coated vesicles from pig brain. Because the reductions by Stelazine in both coated surface and coated vesicle formation are roughly proportional, we have assumed that Stelazine does not significantly affect other processes in the coated vesicle pathway of receptor-mediated endocytosis (Fig. 7). A consequence of this assumption is that the significant reduction in the ferritin-labeled membrane seen in the large vesicular compartment after 15 min of Stelazine treatment is the result of inhibition of the postulated alternate pathway. Thus, pinocytosis in general may be calmodulin regulated.



## Involvement of Actin in Receptor Redistribution and Endocytosis

Our morphometric analysis indicates that the coated vesicle-mediated internalization of cell surface immunoglobulin is sensitive to dhCB. In our study, dhCB treatment results in a complete inhibition of capping and a reduction in the number of coated vesicles containing ferritin label. This drug has little or no effect on the recruitment of coat material to the cell membrane opposite ferritin clusters and reduces only slightly the alternate endocytic pathway. These results implicate the actin microfilament system in (a) capping, but not in clustering or patching of receptors (in accord with other investigators [12, 46]), and (b) conversion of coated pits into coated vesicles. Our observations of HMM-decorated filaments in direct association with uncoated plasma membrane below ligand-receptor complexes support the role of actin microfilaments in capping (12, 46). The association of HMM-decorated filaments with clathrin-coated pits and vesicles is evidence of an active role of actin microfilaments in the formation of coated vesicles.

Evidence for recruitment and/or assembly of actin filaments to capping cell surface determinants is accumulating. Co-capping of actin and myosin with cross-linked cell surface determinants has been observed (8). In addition, Flanagan and Koch (14) have demonstrated an association of cross-linked surface Ig and cytoplasmic actin in lymphocytes and P3 myeloma cells. Furthermore, a dynamic association of actin and myosin with capping concanavalin A receptors of *Dictyostelium* has been shown recently by one of us (12).

In contrast to the apparent role of microfilaments in lateral movement of membrane surface receptors, their involvement in endocytosis is less clear (for example, see references 4, 48, 51). Earlier reports of failure of cytochalasin B to inhibit endocytosis, even along a pathway involving coated vesicles (e.g., 51) must be reinterpreted in light of our findings. Clearly, given enough time in our system, a portion of endocytosis of labeled ligand will occur via coated vesicles even in the presence of dhCB, because it is the rate of coated vesicle formation that is affected, not the entry of label into the coated membrane pathway. Because the alternate pathway is little affected by cytochalasin (at the concentration we have employed), perhaps in the presence of the drug a different equilibrium would be established so that some labeled ligand in coated pits would eventually be endocytosed via the alternate pathway.

Just how dhCB prevents coated vesicle formation is undetermined. We score independent, fully coated membrane profiles in the cell cytoplasm as coated vesicles. We have not determined in each case that these are totally free from the cell surface; perhaps some of them are connected via a long channel as seen in Fig. 3c. This may mean that actin attached to the coated pit pulls the surface inward to form such deep channels, at which time a rearrangement of the coat material completes the vesiculation, as suggested by others (22).

In our observations of microfilament associations with coated membranes, the arrowhead polarity of HMM decoration points into the cytoplasm, away from the membrane. This polarity appears to be constant and is similar to that seen elsewhere (35, 47). Sometimes, actin filaments from different places on the membrane are connected by "thick filaments" in the manner predicted by Spudich (44) as in Fig. 4b. This orientation might be expected for active involvement of microfilaments in pulling the coated membrane into the cytoplasm.

Additional evidence for active linkage between actin and

clathrin-coated vesicles is shown in Fig. 6. Isolated coated vesicle fractions contain, as their principal components, polypeptides that comigrate with authentic brain clathrin and rabbit muscle actin. The amount of actin relative to clathrin varies, suggesting that the association is somewhat labile or dynamic.

## A $Ca^{2+}$ Signal in Endocytosis?

The suggestion that calmodulin is associated with early events such as coat recruitment in receptor-mediated endocytosis via the coated vesicle pathway as well as the alternate pathway, and that actin interactions may provide the motive force for events such as capping and coated vesicle internalization tempts us to postulate that endocytosis begins with a transient flux of  $Ca^{2+}$  beneath the cell membrane. Is receptor-ligand clustering then equivalent to  $Ca^{2+}$  channel formation?  $Ca^{2+}$  binding to calmodulin at the cytoplasmic surface of the membrane might activate enzymes such as adenylate cyclase, phosphodiesterase, and myosin light chain kinase (11), among others. We may then ask which, if any, of these enzymes is associated with clathrin binding to the membrane, with subsequent activation of the actin microfilament system, and so forth. Myosin light chain kinase would be a suitable candidate enzyme that might link the Stelazine-sensitive step to the later dhCB-sensitive step, because actin-myosin interaction is envisioned as providing the motile mechanism for capping and for coated vesicle formation.

The authors thank Dr. B. Bloom for providing the WiL2 stock and his assistance and instruction on cell culture. We are grateful to Dr. S. Lin for the dihydrocytochalasin B and to Dr. A. Means for the calmodulin standard.

This work was supported by grants from the American Cancer Society (BC-302) and the U.S. Public Health Service (USPHS) (GM 25813) to J. S. Condeelis and USPHS (HL 22560) to P. Satir.

J. S. Condeelis is a Rita Allen Foundation Scholar. J. L. Salisbury is a Leukemia Society of American Fellow.

A portion of this work was presented at The American Society for Cell Biology meeting in Toronto, Canada, in November 1979 (42).

Received for publication 14 April 1980, and in revised form 11 June 1980.

## REFERENCES

1. Ainsworth, S. K., and M. J. Karnovsky. 1972. An ultrastructural staining method for enhancing the size and electron opacity of ferritin in thin sections. *J. Histochem. Cytochem.* 20:225-229.
2. Albertini, D. F., R. D. Berlin, and J. M. Oliver. 1977. The mechanism of concanavalin A cap formation in leukocytes. *J. Cell Sci.* 26:57-75.
3. Albertini, D. F., and J. I. Clark. 1975. Membrane-microtubule interactions: concanavalin A capping induced redistribution of cytoplasmic microtubules and colchicine binding proteins. *Proc. Natl. Acad. Sci. U. S. A.* 72:4976-4980.
4. Allison, A. C., P. Davies, and S. DePetris. 1971. Role of contractile microfilaments in macrophage movement and endocytosis. *Nature New Biology.* 232:153-155.
5. Anderson, R. G. W., E. Vasilie, R. J. Mello, M. S. Brown, and J. L. Goldstein. 1978. Immunocytochemical visualization of coated pits and vesicles in human fibroblasts: relation to low density lipoprotein receptor distribution. *Cell.* 15:919-933.
6. Begg, D. A., R. Rodewald, and L. I. Rebhun. 1979. The visualization of actin filament polarity in thin sections: evidence for the uniform polarity of membrane-associated filaments. *J. Cell Biol.* 79:846-852.
7. Bolton, A. E. 1977. Radioiodination techniques. Review 18. Amersham Corporation, Arlington Heights, Ill. 71.
8. Bourguignon, L. Y. W., K. T. Tokuyasu, and S. J. Singer. 1978. The capping of lymphocytes and other cells, studied by an improved method of immunofluorescence staining of frozen sections. *J. Cell Physiol.* 95:239-258.
9. Brenner, S. L., and E. D. Korn. 1979. Substoichiometric concentrations of cytochalasin D inhibit actin polymerization. *J. Biol. Chem.* 254:9982-9985.
10. Brown, S. S., and J. A. Spudich. 1979. Cytochalasin inhibits the rate of elongation of actin filaments. *J. Cell Biol.* 83:657-662.
11. Cheung, W. Y. 1980. Calmodulin plays a pivotal role in cellular regulation. *Science (Wash. D. C.)* 207:19-27.
12. Condeelis, J. S. 1979. Isolation of concanavalin A caps during various stages of formation and their association with actin and myosin. *J. Cell Biol.* 80:751-758.
13. DePetris, S., and M. C. Raff. 1973. Normal distribution, patching and capping of surface immunoglobulin studied by electron microscopy. *Nature New Biol.* 241:257-259.

14. Flanagan, J., and G. L. E. Koch. 1978. Cross-linked surface Ig attaches to actin. *Nature (Lond.)* 273:278-281.
15. Fox, C. F., and M. Das. 1979. Internalization and processing of the EGF receptor in the induction of DNA synthesis in cultured fibroblasts: the endocytic activation hypothesis. *J. Supramol. Struct.* 10:199-214.
16. Goldstein, J. C., R. G. W. Anderson, and M. S. Brown. 1979. Coated pits, coated vesicles, and receptor mediated endocytosis. *Nature (Lond.)* 279:679-685.
17. Gordon, P., J. L. Carpentier, S. Cohen, and L. Orci. 1978. Epidermal growth factor: morphological demonstration of binding, internalization, and lysosomal association in human fibroblasts. *Proc. Natl. Acad. Sci. U. S. A.* 75:5025-5029.
18. Helenius, A., J. Kartenbeck, K. Simons, and E. Fries. 1980. On the entry of Semliki Forest virus into BHK-21 cells. *J. Cell Biol.* 84:404-420.
19. Hidaka, H., T. Yamaki, T. R. Totsuka, and M. Asano. 1979. Selective inhibition of Ca<sup>2+</sup>-binding modulator of phosphodiesterase produces vascular relaxation and inhibits actin-myosin interaction. *Mol. Pharmacol.* 15:49-59.
20. Ishikawa, H., M. Bischoff, and H. Holtzer. 1969. Formation of arrowhead complexes with heavy meromyosin in a variety of cell types. *J. Cell Biol.* 43:312-328.
21. Jett, M., and C. Hickey-Williams. 1977. Lymphoid cells in mammalian cell membranes. *Surface Membranes of Specific Cell Types*. Vol. 3. G. A. Jamieson and D. M. Robinson, editors. Butterworth & Co., London. 47-88.
22. Kanaseki, T., and K. Kadota. 1969. The "vesicle in a basket": a morphological study of coated vesicle isolated from nerve endings of the guinea pig brain, with special reference to the mechanism of membrane movements. *J. Cell Biol.* 42:202-220.
23. Keen, J. H., M. D. Willingham, and I. H. Pastan. 1979. Clathrin-coated vesicles: isolation, dissociation and factor-dependent reassociation of clathrin baskets. *Cell* 16:303-312.
24. Kennel, S. J., and R. A. Lerner. 1973. Isolation and characterization of plasma membrane associated immunoglobulin from cultured human diploid lymphocytes. *J. Mol. Biol.* 76:485-502.
25. Laemmli, U. K. 1970. Cleavage of structural proteins during the assembly of the head of bacteriophage T4. *Nature (Lond.)* 227:680-685.
26. Lerner, R. A., P. J. McConahey, and F. J. Dixon. 1971. Quantitative aspects of plasma membrane-associated immunoglobulin in clones in diploid human lymphocytes. *Science (Wash. D. C.)* 173:6-62.
27. Levin, R. M., and B. Weiss. 1976. Mechanism by which psychotropic drugs inhibit adenosine cyclic 3',5'-monophosphate phosphodiesterase of brain. *Mol. Pharmacol.* 12:581-589.
28. Levy, J. A., M. Virolainen, and U. Defenoli. 1968. Human lymphoblastoid lines from lymph node and spleen. *Cancer (Phila.)* 22:517-524.
29. Lin, S., D. C. Lin, and M. D. Flanagan. 1978. Specificity of the effects of cytochalasin B on transport and motile processes. *Proc. Natl. Acad. Sci. U. S. A.* 75:329-333.
30. Lin, D. C., K. D. Tobin, M. Grumet, and S. Lin. 1980. Cytochalasins inhibit nuclei induced actin filament polymerization by blocking filament elongation. *J. Cell Biol.* 84:455-460.
31. Lin, S., and C. E. Snyder, Jr. 1977. High affinity cytochalasin B binding to red cell membrane proteins which are unrelated to sugar transport. *J. Biol. Chem.* 252:5464-5471.
32. Linden, C. D., T. F. Roth, and J. R. Dedman. 1979. The association of calmodulin with coated vesicles. *J. Cell Biol.* 83:289a (Abstr.).
33. Lowey, S., and C. Cohen. 1962. Studies on the structure of myosin. *J. Mol. Biol.* 7:293-308.
34. Maxfield, F. R., J. Schlessinger, Y. Schechter, I. Pastan, and M. C. Willingham. 1978. Collection of insulin, EGF and  $\alpha_2$ -macroglobulin in the same patches on the surface of cultured fibroblasts and common internalization. *Cell* 14:805-810.
35. Mooseker, M. S., and L. G. Tilney. 1976. Organization of actin filament-membrane complex: filament polarity and membrane attachment in the microvilli of intestinal epithelial cells. *J. Cell Biol.* 67:724-743.
36. Nossel, G. J. J. 1977. B-lymphocyte receptors and lymphocyte activation. In *International Cell Biology 1976-1977*. B. R. Brinkley and K. R. Porter, editors. The Rockefeller University Press, New York. 107-111.
37. Novikoff, A. 1973. Lysosomes: a personal account. In *Lysosomes and Storage Diseases*. G. Hers and F. Van Hoof, editors. Academic Press, Inc., New York. 1-41.
38. Pearse, B. M. F. 1975. Coated vesicles from pig brain: purification and biochemical characterization. *J. Mol. Biol.* 97:93-98.
39. Poste, G., D. Papahadjopoulos, and G. L. Nicolson. 1975. Local anesthetics affect transmembrane cytoskeletal control of mobility and distribution of cell surface receptors. *Proc. Natl. Acad. Sci. U. S. A.* 72:4430-4434.
40. Roth, T. F., J. A. Cutting, and S. B. Atlas. 1976. Protein transport: a selective membrane mechanism. *J. Supramol. Struct.* 4:527-548.
41. Roth, R. F., and K. R. Porter. 1964. Yolk protein uptake in the oocyte of the mosquito, *Aedes aegypti*. *J. Cell Biol.* 20:313-332.
42. Salisbury, J. L., J. S. Condeelis, and P. Satir. 1979. Microfilaments and clathrin play a direct role in endocytosis of crosslinked cell surface immunoglobulin. *J. Cell Biol.* 83:72a (Abstr.).
43. Singer, S. J., J. F. Ash, L. Y. W. Bourguignon, M. H. Heggeness, and D. Louvard. 1978. Transmembrane interactions and the mechanism of transport of proteins across membranes. *J. Supramol. Struct.* 9:373-389.
44. Spudich, J. A. 1974. Biochemical and structural studies of actomyosin-like proteins from non-muscle cells. II. Purification, properties and membrane association of actin from amoebae of *Dictyostelium discoideum*. *J. Biol. Chem.* 249:6013-6020.
45. Steinman, R. M. 1976. Horseradish peroxidase as a marker for studies of pinocytosis. In *In Vitro Methods of Cell-Mediated and Tumor Immunity*. B. R. Bloom and J. R. David, editors. Academic Press, Inc., New York. 379-386.
46. Taylor, R. B., W. Duffus, M. Raff, and S. DePetris. 1971. Redistribution and pinocytosis of lymphocyte surface immunoglobulin molecules induced by anti-immunoglobulin antibody. *Nature New Biology* 233:225-229.
47. Tilney, L. G. 1975. The role of actin in non-muscle cell motility. In *Molecules and Cell Movement*. S. Inoué and R. E. Stephens, editors. Raven Press, New York. 339-388.
48. Wagner, R., M. Rosenberg, and R. Estensen. 1971. Endocytosis in Chang liver cells: quantitation by sucrose-<sup>3</sup>H uptake and inhibition by cytochalasin B. *J. Cell Biol.* 50:804-817.
49. Weibel, E. R. 1969. Stereological principles for morphometry in electron microscopic cytology. *Int. Rev. Cytol.* 26:325-307.
50. Weiss, B., and R. M. Levin. 1978. Mechanism for selectively inhibiting the activation of cyclic nucleotide phosphodiesterase and adenylate cyclase by antipsychotic agents. *Adv. Cyclic Nucleotide Res.* 9:285-304.
51. Wills, E. J., P. Davis, A. C. Allison, and A. D. Haswell. 1972. Cytochalasin B fails to inhibit pinocytosis by macrophages. *Nature New Biology* 240:58-60.